Effects of SiC Whiskers and Particles on Precipitation in Aluminum Matrix Composites

JOHN M. PAPAZIAN

The age-hardening precipitation reactions in aluminum matrix composites reinforced with discontinuous SiC were studied using a calorimetric technique. Composites fabricated with 2124, 2219, 6061, and 7475 alloy matrices were obtained from commercial sources along with unreinforced control materials fabricated in a similar manner. The 7475 materials were made by a casting process while the others were made by powder metallurgy: the SiC reinforcement was in the form of whiskers or particulate. It was found that the overall age-hardening sequence of the alloy was not changed by the addition of SiC, but that the volume fractions of various phases and the precipitation kinetics were substantially modified. Precipitation and dissolution kinetics were generally accelerated. A substantial portion of this acceleration was found to be due to the powder metallurgy process employed to make the composites, but the formation kinetics of some particular precipitate phases were also strongly affected by the presence of SiC. It was observed that the volume fraction of GP zones able to form in the SiC containing materials was significantly reduced. The presence of SiC particles also caused normally quench insensitive materials such as 6061 to become quench sensitive. The microstructural origins of these effects are discussed.

I. INTRODUCTION

ALUMINUM alloys reinforced with whisker or particulate SiC are attractive for applications requiring higher stiffness and strength than traditional aluminum alloys. Because the reinforcing phase is discontinuous, these "short fiber reinforced composites" (SFRC) are similar to conventional aluminum alloys in that they are nearly isotropic and can be processed and formed by traditional metalworking techniques.[1] These advantages, coupled with a potential low cost, have led to rapid commercialization, and SFRC aluminum alloys are now available from three commercial sources. The original fabrication process was based on a powder metallurgy (PM) technique,[2] but an ingot metallurgy (IM) process has been developed so that both PM and IM materials are now available.[3]

Unlike continuous filament composites, the properties of the matrix alloy of an SFRC play a significant role in the yield strength of the composite. To date, the matrix alloys of choice have been the age-hardenable alloys 2124, 6061, and 7475. The strength increment due to age-hardening is necessary in order to develop acceptable properties. For example, Arsenault found that adding 20 pct SiC to annealed 6061 increased the yield strength by 100 MPa,[4] but heat treating unreinforced 6061 from the annealed condition to T6 increased the yield strength by 220 MPa.[5] (The original, annealed value is 55 MPa.[5]) Thus, the strength increment due to age-hardening is greater than or equal to the strengthening due to the introduction of SiC and must be considered when explanations for the mechanical behavior of these materials are sought.

The strengthening whiskers or particles employed to make SFRC are typically high melting point, relatively inert phases such as SiC, B_4C, and Al_2O_3, and they are not expected to modify significantly the overall chemistry of the matrix aluminum alloy. To a first approximation, they are thought of as inert with respect to the age-hardening precipitation reactions. However, preliminary investigations have shown that there are effects of the reinforcing particles on precipitation in the matrix. Nieh and Karlak have shown that B_4C particles affect the aging behavior of B_4C reinforced 6061.[6] They found that the composite reached peak hardness in 3 hours at 450 K while a control PM alloy took 10 hours. They attributed this acceleration to the presence of high diffusivity paths in the composite, particularly the dislocations introduced by differential thermal expansion, and the particle matrix interfaces. Similar acceleratory effects of SiC in various aluminum alloy matrices are generally recognized, but specific results do not seem to have been published. Thus, the state of matrix precipitation is significant to the mechanical properties of SFRC, and the presence of the reinforcing phase influences the matrix precipitation, so an investigation of these relationships is important for understanding the behavior of SFRC materials. The logical first step in this effort should be an evaluation of the effects of the reinforcing phase on matrix precipitation.

Transmission electron microscopy has been applied to this question. A detailed examination of the phase distribution in 15 pct SiC/2124 was performed by Nutt and Carpenter.[7] Their samples had a 0.5 to 2.0 μm grain size and a *low* density of mobile dislocations in the matrix. They observed various large (1 to 5 μm) constituent particles, generally associated with SiC whiskers, and widespread 0.2 to 1.0 μm dispersoid particles. Both of these categories of particles were larger than typically observed in the base alloy: this was thought to be a consequence of processing above the solidus, as is typical for PM SFRC. They found numerous small (10 nm) MgO particles at the Al-SiC interface, and they also observed significant segregation of magnesium to the interface. (In contrast to the magnesium segregated layer observed at the SiC-Al interface in SiC/2124, Nutt found a 3 nm thick, continuous layer of polycrystalline oxide at the SiC-Al interface in

JOHN M. PAPAZIAN is Principal Staff Scientist with Grumman Corporate Research Center, A01-26 Bethpage, NY 11714-3580.

Manuscript submitted November 13, 1987.

SiC/6061 composites.[8]) With respect to the age-hardening precipitates, Nutt and Carpenter commonly observed 20 to 80 nm S phase precipitates at the grain boundaries.[7] These precipitates were at the smaller end of the size range after a room temperature aging treatment and at the upper end after 190 °C aging. In the grain interiors they found S′ precipitates that were larger than typical for the aging employed. They also noted that the distribution of S′ was not homogeneous, with some grains containing numerous precipitates while neighboring grains had very few.

In addition to the above described characterization of precipitation, the effects of SiC particles or whiskers on other aspects of the matrix microstructure of SFRC have been the subject of several investigations. Arsenault and Fisher observed a high ($4 \times 10^{14}/m^2$) density of dislocations clustered around the ends of SiC whiskers and forming low angle cell boundaries in a 20 pct SiC_w/6061 composite.[9] They also observed very fine precipitates along the dislocations. Subsequently, the generation of these dislocations was observed *in situ* using a hot stage in an HVEM.[10] These observations were explained by the large, approximately 10:1, difference in the thermal expansion coefficient between SiC and Al. This causes a differential expansion or contraction during heating and cooling and leads to the generation of dislocations. Additional experiments allowed identification of individual Burgers vectors and the development of a theory based on prismatic punching.[11,12] Using a model system of a single SiC fiber embedded in an aluminum matrix, Flom and Arsenault were able to show that the extent of the zone in which dislocation motion occurred was approximately equal to the theoretical plastic zone size and that the size of this dislocation filled region decreased somewhat as the cooling rate from the solution treatment temperature increased.[13] The work described above has shown that the presence of SiC whiskers or particles in aluminum alloy matrices results in the generation of a large number of dislocations during cooling from elevated temperatures. The presence of these dislocations can significantly affect the properties of the matrix, and it is Arsenault's view that dislocation strengthening is the predominant effect of the SiC additions on the mechanical properties of these materials.[14] An additional microstructural effect of the presence of SiC is the development of a small residual tensile stress in the aluminum matrix.[15]

In light of the results described above, and of the emerging view of the importance of the matrix microstructure to the properties of SFRC,[16,17] it was thought that an investigation of the effects of SiC reinforcements on the age-hardening reactions in commercial aluminum alloys would be appropriate. A calorimetric technique was selected for these experiments in order to complement the detailed TEM work described above. The calorimetric technique allows rapid evaluation of the possible effects of the reinforcement on the identity of the phases present, on precipitate volume fractions, and on reaction kinetics. Composites fabricated from a variety of matrix alloys were employed, and, because the PM process has been implicated in some of the observed microstructural effects, SFRC prepared using the ingot metallurgy approach were also examined.

II. EXPERIMENTAL PROCEDURE

The composite materials for these experiments were obtained from several sources and were fabricated by both powder metallurgy and ingot casting techniques. Four matrix alloys were employed: 2124, 2219, 6061, and 7475. The first three were powder metallurgy materials, whereas the composites based on 7475 were made by a casting technique. The characteristics of each material are listed in Table I.

The F9 SiC is a whisker grade manufactured by Arco Chemicals Corp., Greer, SC, and, according to the manufacturer, the starting material has a mean whisker diameter of 0.52 μm and a mean length of 13 μm. The whiskers are broken during powder mixing, compaction, and extrusion. Measurements on our 20 pct SiC_w/2124 material in the as-extruded condition showed an average aspect ratio of approximately 3; thus the average length was reduced to approximately 1.5 μm.[18] The 2124 composites had all been hot extruded by the manufacturer from a 75 mm diameter billet to 16 mm diameter bar. The 2219 composites had been extruded to 12.7 mm by 100 mm. The 6061 composites were fabricated by the Naval Surface Weapons Center, White Oak Laboratory, Silver Spring, MD, and had been extruded to 9.5 mm diameter rods from 125 gm billets. The 7475 composites were fabricated by SAI International (currently, Dural Aluminum Composites Corp.[3]), using a proprietary casting technique. The SiC particulate used was a commercial grade grinding compound with an irregular shape and a characteristic dimension of approximately 10 μm. The billets were hot extruded from 75 mm diameter to a 16 mm by 38 mm rectangular cross section. For all of the alloys, control samples taken from commercially produced extrusions were also used to provide an ingot metallurgy baseline.

Samples for DSC analysis were machined by conventional techniques from the various starting materials. The 2124, 2219, and 7475 samples were in the form of small discs or rectangular plates that were 1.6 mm thick. The 6061 samples were in the form of 6.4 mm diameter by 25 mm long cylinders. The samples were heat treated in a vertical tube furnace with an argon atmosphere and were quenched by dropping from the furnace directly into an ice brine solution or boiling water. Cooling rates were measured by embedding 0.5 mm diameter thermocouples in the cylindrical 6061 samples. Results of these tests showed that the average cooling rate in the temperature interval from 400 °C to 290 °C was 1400 K/s for ice brine, 18.5 K/s for boiling water, and 2.5 K/s for air cooling. Simple heat transfer calculations indicate that the 1.6 mm plate-like samples should have cooled approximately twice as fast.

Table I. Experimental Materials

Matrix	SiC Type	Volume Pct	Supplier	Method
2124	F9	0, 8, 20	Arco	powder
2219	F9	0, 20	Arco	powder
6061	F9	0, 20	NSWC	powder
7475	10 μm particulate	0, 10, 15	SAI	ingot

The solution treatment temperatures employed were 520 °C for 2124, 535 °C for 2219, 530 °C for 6061, and 482 °C for 7475. Solution treatment times were typically one hour. Samples that were to be analyzed in the as-quenched condition were immediately stored in liquid nitrogen while the T4 materials were allowed to age at room temperature. Elevated temperature aging was performed in oil baths.

DSC analysis was performed using DuPont 990 and R99 thermal analyzers with plug-in DSC modules. The experimental technique has been previously described.[19] The heating rate was 10 K/min. DSC discs, 5.6 mm in diameter, were punched from the heat treated samples using a specially ground punch to minimize distortion. At least three DSC runs were typically made for each heat treat condition. In SiC containing material, all of the DSC curves and reaction enthalpies were normalized so that they refer only to the mass of the aluminum alloy matrix. The SiC contribution was removed. The results are plotted as heat capacity, C_p, *vs* temperature, T, curves or as differential heat capacity, ΔC_p, *vs* temperature. The differential heat capacity was obtained by subtracting the background heat capacity of the matrix from the C_p data, thus leaving only the excess heat capacity due to solid state reactions occurring during the DSC run.[19] The important aspects of the DSC results are the locations and areas of the reaction peaks. Vertical shifts of the C_p *vs* T curves are a result of small errors in the calorimetric measurement and are not significant for these experiments.

III. RESULTS

Precipitation reactions in age-hardening aluminum alloys are most visible in DSC scans when the material is in an as-quenched (W) condition. The DSC experiment is started at approximately 0 °C, and most of the primary precipitation and dissolution reactions occur as the experiment proceeds to the solution treatment temperature. These reactions are easily visible on the thermogram and provide an overall view of the precipitation and dissolution processes in the sample. Thus, all of the composite materials were surveyed in the W condition. As discussed below, it was found that some of these materials were quench sensitive, so efforts were made to insure that all of the samples were quenched as rapidly as possible.

A. *As-Quenched Microstructures*

Results from DSC scans of the 8 pct SiC_W/2124 and 20 pct SiC_W/2124 composites are shown in Figure 1. For comparison purposes, results from a powder metallurgy 2124 alloy which was prepared using the same powder and process as the composites are also shown in Figure 1, along with results from an ingot metallurgy extrusion of 2124. Curves from all four of the materials show the same general features: an exotherm between 25 °C and 150 °C due to the formation of GPB zones; an endotherm between 150 °C and approximately 245 °C due to the dissolution of GPB zones; an exotherm between 245 °C and 310 °C due to the formation of S′; and an endotherm between 310 °C and 520 °C due to the dissolution of S′. Thus, the overall characteristics of the age-hardening reactions in 2124 are not changed

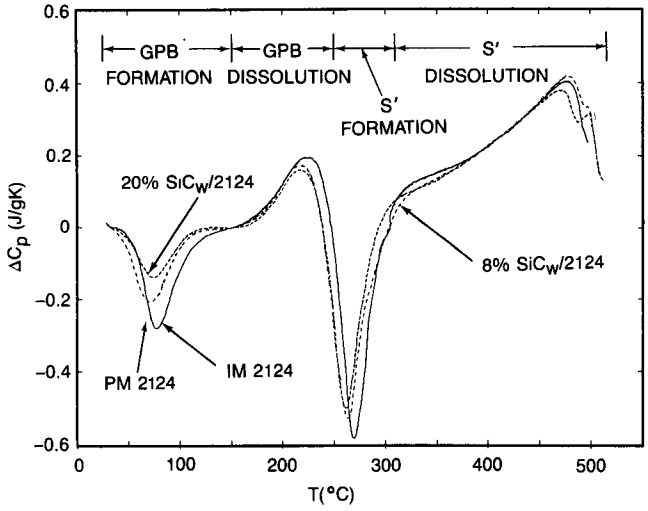

Fig. 1—Comparison of the precipitation reactions in wrought 2124 (solid line), powder metallurgy 2124 (dotted line), 8 pct SiC_W/2124 (dot-dashed line), and 20 pct SiC_W/2124 (dashed line). All of the materials are in an as-quenched (W) condition.

by the addition of SiC, but some aspects of the reactions are altered. The curves in Figure 1 show that the areas and the peak temperatures of the first three reactions in the composite material are decreased relative to those of the ingot metallurgy material. The area of the peak gives the reaction enthalpy, which is directly related to the molar heat of reaction and the volume fraction of the precipitating or dissolving phase,[20] while the temperature is related to the size and stability of the precipitate and to the reaction kinetics.[20–23] The extent of the changes can be seen in Table II, where the reaction enthalpies and peak temperatures are tabulated.

The data in Table II show that the temperatures of the first three peaks are lower in the PM material and the two composites relative to the IM material. This is interpreted to mean that the formation and dissolution kinetics of these phases are accelerated by some aspect of the powder metallurgy process used in their preparation. It is important to note that this acceleration occurred in all three of the PM materials, not just the SiC containing composites. Within the limits of the standard deviation, the reaction enthalpy of the S′ formation peak is the same in all four materials, but the GPB zone formation and dissolution reactions are less energetic in the SiC containing materials. This indicates that fewer GPB zones form and dissolve in the composites. The volume fraction of GPB zones present in the 20 pct SiC composite is approximately 40 pct less than that in the IM and PM materials. These results indicate that there are two differences between the 2124 IM baseline material and the composites: an enhancement of the precipitation kinetics by some microstructural aspect of the powder metallurgy process, and a diminution of the volume fraction of GPB zones caused by the presence of SiC whiskers.

Results from the DSC scans of the 2219 materials are shown in Figure 2, and the reaction temperatures and enthalpies are tabulated in Table II. For this alloy, the IM material shows five reactions whose temperature ranges are identified on the figure.[22] The powder metallurgy material shows the same general reactions, but the 20 pct SiC_W/2219 composite is significantly different in the high temperature

Table II. Effects of SiC on Precipitation in the As-Quenched Condition

	GP Zone Phase				Intermediate Phase			
	Formation		Dissolution		Formation		Dissolution	
Alloy	T, °C	ΔH, J/g	T, °C	ΔH, J/g	T, °C	ΔH, J/g	T, °C	ΔH, J/g
IM 2124	78	− 9.9	223	10.0	268	−14.6		
PM 2124	67	−10.4	217	7.5	263	−14.9		
8 pct SiC/2124	72	− 8.5	219	6.7	264	−15.8		
20 pct SiC/2124	71	− 6.0	218	5.9	262	−14.1		
IM 2219			151	4.2	279	−18.9		
PM 2219			146	4.5	300	−12.6		
20 pct SiC/2219			144	1.6	264	−16.6	SA	SA
IM 6061					239, 289			
PM 6061					230, 285			
20 pct SiC/6061					225, 271		SA	SA
IM 7475	88	− 8.6			232	−15.6	422	22.6
Cast 7475	89	− 9.3			233	−14.4	411	22.5
10 pct SiC/7475	86	− 4.8			227	−14.8	408	22.8
15 pct SiC/7475	87	− 6.1			230	−13.9	410	22.6

Std. dev. of T is ±1 °C; std. dev. of H is ±10 pct; and SA = significantly altered.

θ formation and dissolution reactions. The 20 pct SiC_w/2219 curve never returned to the baseline, indicating that melting of some components of the microstructure probably began at lower temperatures than normal. In addition, GP zone dissolution occurred in the composite at a lower temperature and with a reduced enthalpy compared to IM material. In the PM material, GP zone dissolution also occurred at a lower temperature, but involved approximately the same reaction enthalpy as the IM material. Thus, the powder metallurgy process accelerates GP zone dissolution, but the presence of SiC also reduces the volume fraction of GP zones formed. In this case, the volume fraction of GP zones in the composite is only approximately one-third that of IM material. The θ' formation reaction is also affected. θ' formation is accelerated and attenuated in 20 pct SiC_w/2219 when compared with IM 2219. θ' formation is also significantly altered in the PM material, but the shape of the peak does not lend itself to a simple interpretation.

A comparison between the behavior of IM, PM, and 20 pct SiC_w/6061 is shown in Figure 3. In this alloy system, the high temperature dissolution reactions are altered by the powder metallurgy process and by the presence of SiC, but the microstructural nature of the changes is not clear because a detailed comparison of this thermogram with transmission electron microscopy has not yet been published. Some effects in the intermediate temperature range, however, are apparent. Two formation peaks which occur at 239 °C and 289 °C in the IM material and are tentatively assigned to the formation of β'' and β', respectively, are shifted to lower temperatures. As shown in Table II, the powder metallurgy process shifts the β' peak down approximately 4 °C and the β'' peak down approximately 9 °C.

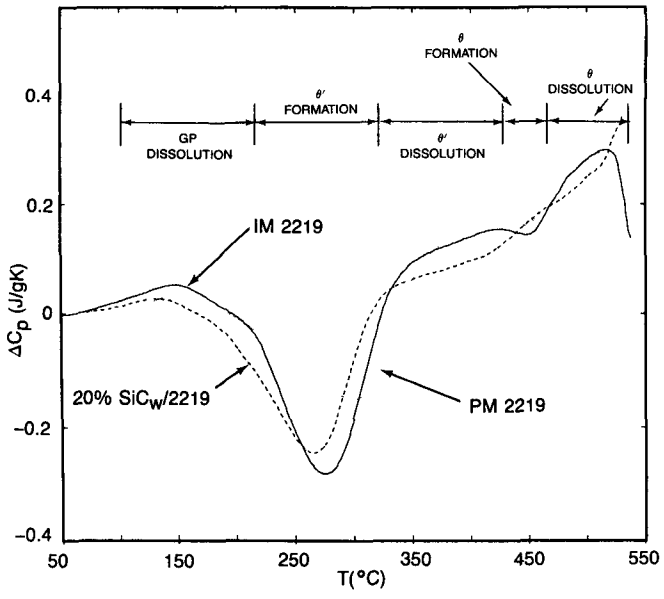

Fig. 2—Comparison of the precipitation reactions in wrought 2219 (solid line), powder metallurgy 2219 (dotted line), and 20 pct SiC_w/2219 (dashed line). All of the materials are in a room temperature aged (T4) condition.

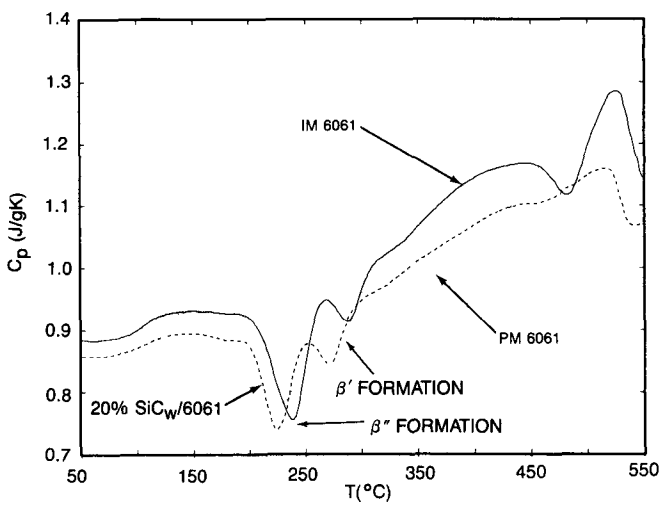

Fig. 3

Fig. 3—Comparison of the precipitation reactions in wrought 6061 (solid line), powder metallurgy 6061 (dotted line), and 20 pct SiC_w/6061 (dashed line). All of the materials are in an as-quenched (W) condition.

Addition of 20 pct SiC_w causes a further acceleration of the reactions by another 14 °C and 5 °C, respectively. Thus, in this case, precipitation of one of the intermediate phases, β'', is accelerated by the PM process and further accelerated by the addition of SiC. Precipitation of the other intermediate phase, β', is slightly accelerated by the PM process, but is very strongly accelerated by SiC. In this alloy, therefore, the relative proportion of the two intermediate precipitate phases present after an elevated temperature aging treatment will be significantly different in the composite when compared to wrought 6061. It is not possible to quantify the reaction enthalpies for these reactions because of the difficulty of finding a suitable baseline, but from visual inspection of the curves, it appears that the volume fractions of β'' and β' are both slightly reduced by the PM process and by the addition of SiC.

Results from the fourth alloy system, 7475, are shown in Figure 4. In the as-quenched condition, the 7475 thermogram consists of a GP zone formation peak followed by η formation and dissolution peaks.[20,23] All of the reactions have similar appearances in the four materials examined: ingot metallurgy 7475, cast 7475, and cast 10 pct and 15 pct SiC_p/7475. Reference to Table II shows that, with the exception of the high temperature dissolution, the peaks occur at approximately the same temperatures in the four materials. The tabulated reaction enthalpy values show that there is no change in the volume fractions of the various phases with the exception of the GP zone formation, which is attenuated by approximately 50 pct. Thus, in these materials, the SiC decreases the volume fraction of GP zones and accelerates the high temperature dissolution of the stable phase. The results from these cast materials are in contrast to those described above, where the powder metallurgy process appeared to cause more extensive microstructural changes.

B. *Effects of Quenching Rate*

Some of the SiC containing composites were found to be more quench sensitive than the parent alloys. An example of this effect is shown in Figure 5, where DSC curves from as-quenched IM 6061 cooled at three quenching rates from

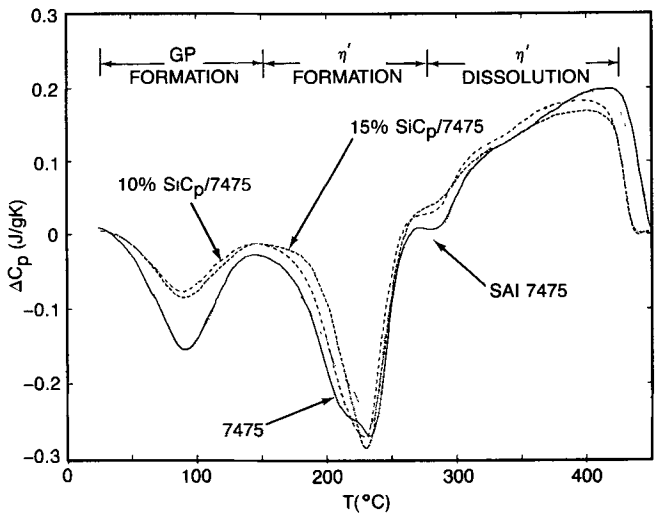

Fig. 4—Comparison of the precipitation reactions in wrought 7475 (solid line), cast 7475 (dotted line), 10 pct SiC_p/7475 (dot-dashed line), and 15 pct SiC_p/7475 (dashed line). All of the materials are in an as-quenched (W) condition.

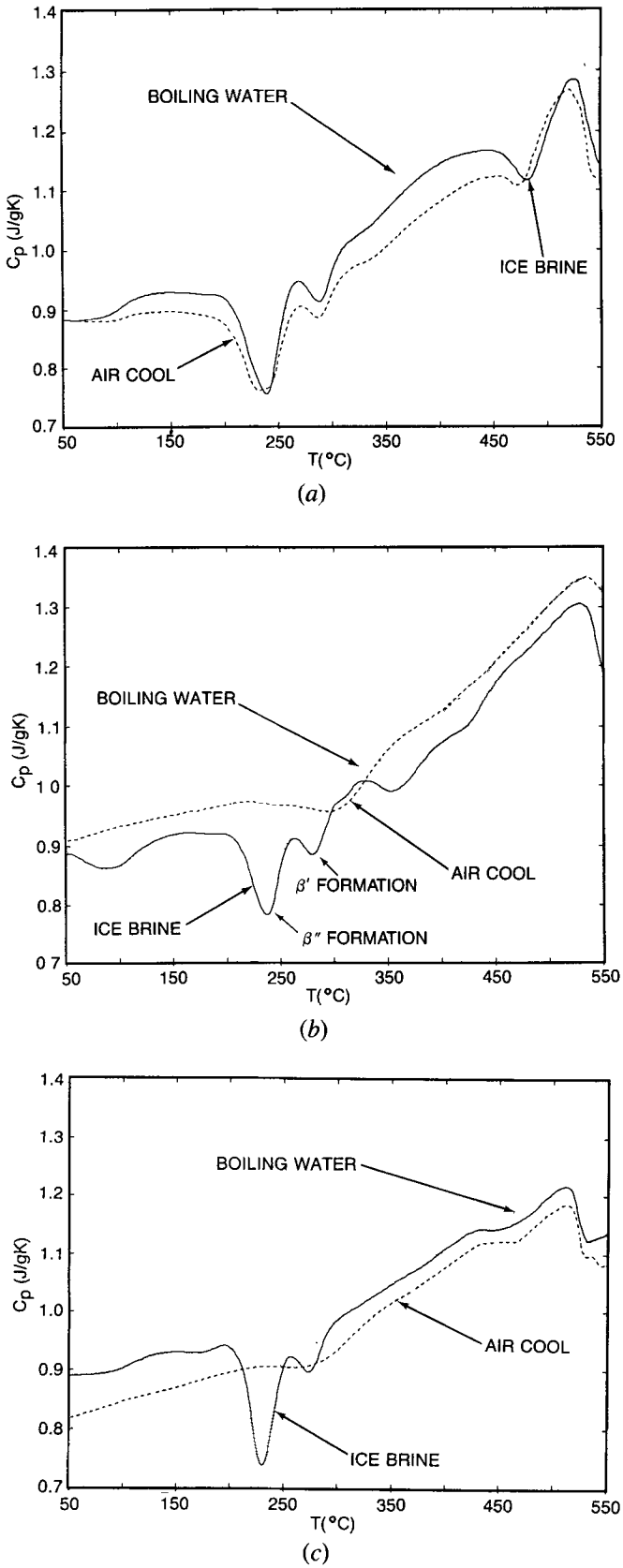

Fig. 5—The effects of cooling at three rates from the solution treatment temperature on (*a*) IM 6061-W, (*b*) PM 6061-W, and (*c*) 20 pct SiC_w/6061-W.

solution treatment are compared with similar curves for PM 6061 and 20 pct SiC_W/6061. The data in Figure 5(a) show that the wrought, ingot metallurgy material displays the same precipitation reactions after ice brine quenching, boiling water quenching, or air cooling. Thus, this material is not quench sensitive. In contrast to this, the data from the composite in Figure 5(c) show a severe attenuation of the intermediate phase formation reactions after a boiling water quench and the near absence of these reactions after air cooling. Data from the PM 6061 material in Figure 5(b) show an intermediate behavior. The reaction enthalpies associated with the curves in Figure 5 are listed in Table III. The tabulated data show that the volume fraction of intermediate phase formed in the IM material decreases only slightly as the cooling rate decreases, but in the SiC_W/6061 composite, air cooling reduces this volume fraction to 20 pct of the rapid quench value. The PM material is less quench sensitive, and shows a significant attenuation of intermediate phase formation only after air cooling. The data in Table III also show that the dissolution enthalpy does not decrease as the quench rate decreases. This shows that, despite the smaller amount of precipitate phase that forms during the DSC runs after the slower quenches, an equivalent amount of precipitate dissolves. This indicates that that precipitate was present in the sample before the DSC run, and thus, it probably formed during the quench. (The delay at room temperature between quenching and DSC analysis was short, typically 15 minutes.) Thus, the reaction enthalpy data show that the presence of SiC in the alloy caused precipitation of approximately 70 pct of the total volume fraction possible of the intermediate phases during the boiling water quench and approximately 80 pct during air cooling. In the PM material very little was formed during the boiling water quench, but approximately 30 pct formed during air cooling.

The results of similar experiments on the 2124 materials are shown in Figure 6. In this system, a boiling water quench of the IM material causes attenuation of GPB zone formation by about 50 pct. (The reaction enthalpies are tabulated in Table IV.) In the 20 pct SiC_W/2124 composite, boiling water quenching causes attenuation of GPB zone formation by approximately 80 pct and also slightly decreases the GPB zone dissolution and S′ formation enthalpies. The PM material behaved like the composite. Thus, most of the possible GPB zones form during a boiling water quench of the composite and the PM alloy, but fewer do so in the IM material. In addition, some S′ forms in the composite and PM material. After air cooling, no GPB zone formation occurred during the DSC scan of any of the materials, but the PM and IM samples showed approximately 30 to 50 pct of their normal GPB zone dissolution enthalpy, while the composite showed very little. Thus some GPB zones formed during air cooling of these materials, with the SiC_W composite having the least. The S′ formation enthalpy was also decreased while S′ dissolution remained unchanged; thus some S′ (approximately 30 pct of the total possible) was also formed during air cooling.

The GP zone dissolution enthalpy and the θ' formation enthalpy observed in IM 2219, PM 2219, and 20 pct SiC_W/2219 are listed in Table V. It can be seen that the volume fractions of GP zones present before the DSC run after the various quenches decrease in roughly the same manner in all three materials as a function of quench rate. Thus, neither the PM process nor the SiC whiskers induce any additional quench sensitivity of GP zones. The θ' formation appears to be slightly more sensitive to quench rate in the composite material than it is in the IM and PM materials, indicating that slightly more θ' is formed during slow quenching of the composite than of the other alloys.

Finally, data from the 7475 alloys are tabulated in Table VI. These data show that all three of the materials have approximately the same quench sensitivity. In each case, boiling water quenching does not have much of an effect, but after air cooling there is no longer any GP zone formation and approximately 50 pct of the intermediate phase has already precipitated. Thus, in this system, the presence of SiC had less of an effect on matrix precipitation behavior than in the other alloys investigated.

IV. DISCUSSION

The first observation to be made from these data is that the introduction of SiC does not substantially modify the age-hardening sequences of these alloys. The same precipitation and dissolution reactions occur in the composites as in the unreinforced materials, and thus the same age-hardening sequences operate. This is a consequence of the lack of rapid reactions between aluminum and SiC when they are both in the solid state and of the absence of extensive reactions during the initial processing and fabrication of the composite. Despite this generalized observation,

Table III. Effects of Quench Rate on Precipitation in 6061-W

Alloy	Quench	Intermediate Phase Formation Enthalpy*	Intermediate Phase Dissolution Enthalpy*
IM 6061	IB	−15.9	16.8
IM 6061	BW	−16.2	16.0
IM 6061	AC	−13.0	16.8
PM 6061	IB	−15.7	13.6
PM 6061	BW	−15.6	16.6
PM 6061	AC	−10.6	17.0
20 pct SiC/6061	IB	−10.6	11.9
20 pct SiC/6061	BW	− 3.3	10.4
20 pct SiC/6061	AC	− 1.9	15.8

* = Joules/gram, standard deviation = ±10 pct.

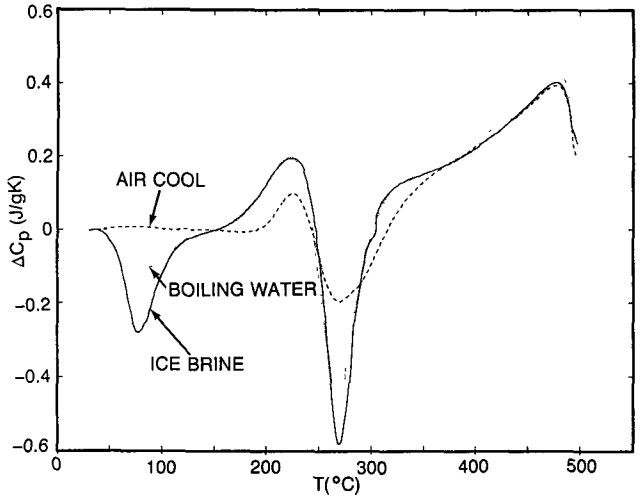

(a)

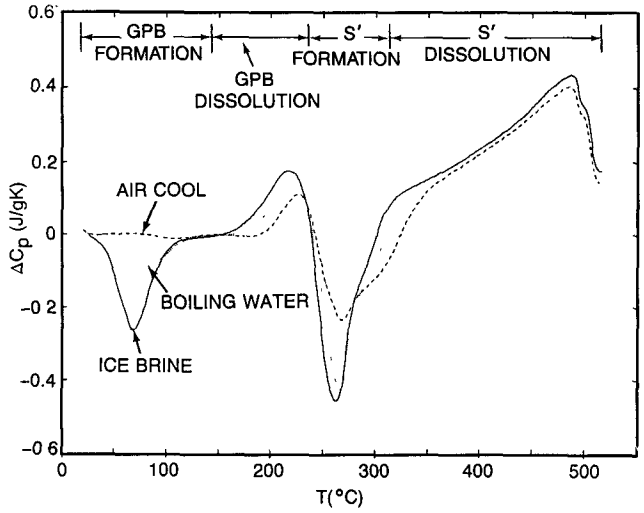

(b)

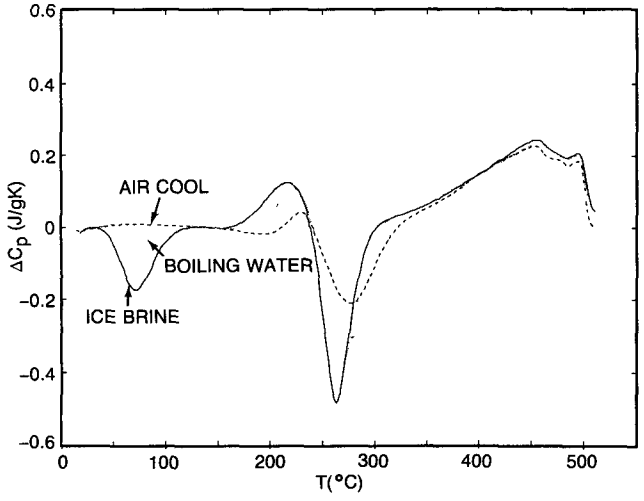

(c)

Fig. 6—The effects of cooling at three rates from the solution treatment temperature on (*a*) IM 2124-W, (*b*) PM 2124-W, and (*c*) 20 pct SiC_w/2124-W.

there are numerous significant effects on the volume fractions of particular phases formed and on the kinetics of formation and dissolution.

With the exception of the 7475 materials, it was generally observed that the kinetics of the GP zone and intermediate phase formation and dissolution reactions were accelerated in the composites. In addition, this acceleration was also observed in the unreinforced PM materials, although it was sometimes less intense. In contrast, the cast 7475 composites and control alloy did not show accelerated precipitation kinetics. These observations indicate that a large part of the acceleratory effect is due to microstructural features introduced by the powder metallurgy preparation process and not to the SiC particles themselves. As pointed out by Nutt,[7] the powder metallurgy process used to prepare these composites differs from the normal one in that it involves consolidation at temperatures that exceed the solidus. This results in the formation of larger constituent and dispersoid particles than otherwise expected.[7] It may also contribute to solute segregation and to formation of the continuous oxide films observed on some SiC particles.[8] In addition, the powder metallurgy process results in a finer grain size and the incorporation of oxide particles. Some or all of these features are thought to be responsible for the enhanced precipitation kinetics.

Not all of the kinetic effects can be attributed to the PM process. In 6061, the PM material showed moderately accelerated β'' and β' formation, but the SiC containing samples showed a pronounced and selective acceleration of β' formation. This can be understood if β' forms on dislocations while β'' does not. Therefore, the enhanced dislocation density in the composite compared to the PM material would accelerate β' formation more than β''. Whatever the mechanism, this observation shows that the relative proportions of β' and β'' will be significantly different in a SiC/6061 composite when compared to IM or PM 6061. This appears to be an unavoidable consequence of the presence of the SiC. The work on B_4C reinforced 6061 showed the effects of this acceleration on the age-hardening curves.[6]

All of the SiC containing materials displayed a reduced volume fraction of GP zones. The volume fractions of the GP zone phases in the composites were approximately one-third to one-half of those in the PM or IM controls. This appears to be an effect specific to the presence of SiC and independent of the preparation process. Since vacancies are usually required to nucleate GP zones and to enhance the room temperature solute diffusivity, it is probable that the operating mechanism involves effects of the SiC particles on the retained vacancy concentration. The likely route for this is thought to be *via* the introduction of a high dislocation density during cooling from solution treatment. The high dislocation density will provide more annihilation sites for retained vacancies, reduce the vacancy content, and thereby reduce the number of GP zones formed.

The presence of SiC causes quench sensitivity in otherwise quench insensitive alloys. The 6061 base alloy could easily be air cooled and still age-harden, but the composite could not even tolerate a boiling water quench. The 2124 composite was also more quench sensitive than the base alloy, but the quench sensitivity of the 2219 and 7475 mate-

Table IV. Effects of Quench Rate on Precipitation in 2124-W

Alloy	Quench	GP Zone Formation Enthalpy*	GP Zone Dissolution Enthalpy*	Intermediate Phase Formation Enthalpy*
IM 2124	IB	− 9.9	10.0	−14.6
IM 2124	BW	− 4.6	8.9	−13.7
IM 2124	AC	0	3.0	− 8.1
PM 2124	IB	−10.4	7.5	−14.9
PM 2124	BW	− 4.4	6.2	−14.8
PM 2124	AC	0	3.2	−10.8
20 pct SiC/2124	IB	− 6.6	5.4	−14.6
20 pct SiC/2124	BW	− 1.2	3.7	−13.1
20 pct SiC/2124	AC	0	0.8	− 9.8

* = Joules/gram standard deviation = ±10 pct.

Table V. Effects of Quench Rate on Precipitation in 2219-W

Alloy	Quench	GP Zone Dissolution Enthalpy*	Intermediate Phase Formation Enthalpy*
IM 2219	IB	4.2	−18.9
IM 2219	BW	2.8	−20.4
IM 2219	AC	0	− 8.5
PM 2219	IB	1.5	−12.6
PM 2219	BW	1.3	−11.6
PM 2219	AC	1.0	− 7.7
20 pct SiC/2219	IB	1.6	−16.6
20 pct SiC/2219	BW	1.5	−10.8
20 pct SiC/2219	AC	0.9	− 5.1

* = Joules/gram, standard deviation = ±10 pct.

Table VI. Effects of Quench Rate on Precipitation in 7475-W

Alloy	Quench	GP Zone Formation Enthalpy*	Intermediate Phase Formation Enthalpy*	Intermediate Phase Dissolution Enthalpy*
cast 7475	IB	−9.3	−14.4	22.5
cast 7475	BW	−8.2	−17.9	21.4
cast 7475	AC	0	− 9.6	23.4
10 pct SiC/7475	IB	−4.8	−14.8	22.8
10 pct SiC/7475	BW	−5.4	−15.7	23.6
10 pct SiC/7475	AC	0	− 6.7	23.7
15 pct SiC/7475	IB	−6.1	−13.9	22.6
15 pct SiC/7475	BW	−6.4	−15.3	23.0
15 pct SiC/7475	AC	0	− 6.5	23.6

* = Joules/gram, standard deviation = ±10 pct.

rials was not exacerbated by SiC. Thus, it appears that highly tolerant alloys, such as 6061, become quench sensitive when SiC is added, but the behavior of relatively intolerant alloys is unchanged. The addition of SiC causes precipitation of GP zones or the intermediate phase during the quench. This is presumed to be due to the presence of numerous heterogeneous nucleation sites in the composites. This was also the case in the PM materials, but to a significantly lesser degree. The microstructural features common to the PM material and the composites are the smaller grain and subgrain size, oxide particles, and larger dispersoid and constituent particles.[7] The additional sites in the composites are the SiC-Al interfaces and the enhanced dislocation density. Nutt has observed heterogeneous nucleation of S phase precipitates at the interface in 2124 composites,[8] so that is a potential mechanism, but the GP zones and intermediate precipitates which precipitate during the quench do not require as potent a nucleation heterogeneity. Thus, their nucleation may be more likely to be affected by the excess dislocations introduced by the SiC particles.

V. SUMMARY

1. The age-hardening sequences in SiC short fiber reinforced composites made with typical commercial

aluminum alloy matrices are similar to those of the unreinforced alloys.
2. The kinetics of GP zone formation and dissolution and intermediate phase formation are accelerated relative to the wrought alloy in both the powder metallurgy control samples and in the SiC containing composites. In addition, the precipitation of particular intermediate phases is further accelerated by the presence of SiC, probably because of the higher dislocation density in the composites.
3. The volume fraction of GP zones formed in the composites is significantly less than that in the powder metallurgy or wrought material. This is thought to be due to a reduced retained vacancy concentration in the composites.
4. The presence of SiC particles, and, to a lesser extent, the powder metallurgy preparation process employed for composite fabrication, causes quench insensitive alloys such as 6061 to become quench sensitive. The more quench sensitive alloys, such as 7475, are not affected.

ACKNOWLEDGMENTS

It is a pleasure to acknowledge the laboratory assistance of Mr. H. Baker and extensive discussions and a critical review of the manuscript by Dr. P. N. Adler. Dr. T. Scott kindly provided the 2219 samples. Portions of this work were supported by the Naval Surface Weapons Center under contract number N60921-82-C-0204, Mr. A. P. Divecha, contract monitor, and by the Air Force Office of Scientific Research under contract number F49620-84-C-0055, Dr. A. Rosenstein, contract monitor. Support was also received from the Grumman Corporation Independent Research and Development Program.

REFERENCES

1. A. P. Divecha, S. G. Fishman, and S. D. Karmarker: *Journal of Metals*, 1981, vol. 33, pp. 12-17.
2. P. J. Lare and A. P. Divecha: U.S. Patent 3,833,697, Sept. 1974.
3. Dural Aluminum Composites Corporation, 10326 Roselle St., San Diego, CA 92121.
4. R. J. Arsenault: *Proc. Japan-U.S. CCM-III*, K. Katawa, S. Umekawa, and A. K. Kobayashi, eds., Tokyo, 1986, pp. 521-27.
5. Aluminum Standards and Data 1978 Metric SI, The Aluminum Association, Washington, DC 20006, p. 32.
6. T. G. Nieh and R. F. Karlak: *Scripta Metall.*, 1984, vol. 18, pp. 25-28.
7. S. R. Nutt and R. W. Carpenter: *Mater. Sci. Eng.*, 1985, vol. 75, pp. 179-77.
8. S. R. Nutt: in "Interfaces in Metal-Matrix Composites," A. K. Dhingra and S. G. Fishman, eds., TMS-AIME, Warrendale, PA, 1986, pp. 157-67.
9. R. J. Arsenault and R. M. Fisher: *Scripta Metall.*, 1983, vol. 17, pp. 67-71.
10. Mary Vogelsang, R. J. Arsenault, and R. M. Fisher: *Metall. Trans. A*, 1986, vol. 17A, pp. 379-89.
11. R. J. Arsenault and N. Shi: *Mater. Sci. Eng.*, 1986, vol. 81, pp. 175-87.
12. M. Taya and T. Mori: *Acta Metall.*, 1987, vol. 35, pp. 155-62.
13. Y. Flom and R. J. Arsenault: *Mater. Sci. Eng.*, 1985, vol. 75, pp. 151-67.
14. R. J. Arsenault: *Mater. Sci. Eng.*, 1984, vol. 64, pp. 171-81.
15. R. J. Arsenault and M. Taya: *Acta Metall.*, 1987, vol. 35, pp. 651-59.
16. J. England and I. W. Hall: *Scripta Metall.*, 1986, vol. 20, pp. 697-700.
17. C. P. You, A. W. Thompson, and I. M. Bernstein: *Scripta Metall.*, 1987, vol. 21, pp. 181-85.
18. W. D. Rooney: Grumman Corp. Research Center, private communication, 1987.
19. J. M. Papazian: *Metall. Trans. A*, 1981, vol. 12A, pp. 269-80.
20. R. J. DeIasi and P. N. Adler: *Metall. Trans. A*, 1977, vol. 8A, pp. 1177-83.
21. P. N. Adler and R. J. DeIasi: *Metall. Trans. A*, 1977, vol. 8A, pp. 1185-90.
22. J. M. Papazian: *Metall. Trans. A*, 1981, vol. 12A, pp. 269-80.
23. J. M. Papazian: *Metall. Trans. A*, 1982, vol. 13A, pp. 761-69.